Fitting Narrow Emission Lines in X-ray Spectra

Taeyoung Park

Department of Statistics, Harvard University

October 25, 2005

X-ray Spectrum

- Quasars are far distant and very luminous objects.
- They emit X-ray luminosity, and the emission of photons with energies is represented by a spectrum.
- The spectrum is characterized by two main components: a continuum term and emission lines.
- The continuum describes a general shape of the spectrum.
- The emission lines are local features in the spectrum and represent extra emission of photons in a narrow band of energy.

Fluorescent Fe-K-alpha Emission Line

- The Fe-K-alpha emission line is the only emission feature identified so far.
- The emission line of the quasar X-ray spectrum is important in the investigation of the state of plasma.
- This line is thought to come directly from illuminated cold accretion flow as a fluorescent process.
- The location of the line indicates the ionization state of iron in the emitting plasma.
- The width of the line tells us the velocity of the plasma.

Quasar PG 1634+706

- PG 1634+706 is a redshift z=1.334 radio quiet and optically bright quasar.
- This source was observed with *Chandra* as a calibration target six times on March 23 and 24, 2000.
- The Fe-K-alpha line has been observed in the quasar rest frame of near 6.4 keV, which corresponds to 2.74 keV in the observed frame of PG 1634+706.

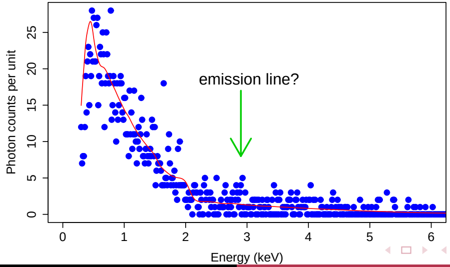

Basic Source Model

- The spectrum is a finite mixture of a continuum term and emission lines.
- We directly model the arrival of photons as an inhomogenous Poisson process, so the expected counts in energy bin j can be modeled as

$$\Lambda_j(\theta) = \Delta_j f(\theta^C, E_j) + \sum_{k=1}^{K} \lambda_k \pi_j(\mu_k, \nu_k).$$

– Δ_j and E_j: the width and mean energy of bin j.

– $f(\theta^C, E_j)$: the expected counts due to the continuum.

– λ_k: the expected counts due to the emission line.

– $\pi(\mu_k, \nu_k)$: the proportion of a line that falls into bin j.

Data Distortion Model

- Data are subject to a number of processes that significantly degrade the source counts:
  - absorption: photons are absorbed by material in the source or between the source and the observer,
  - effective area: stochastic censoring,
  - blurring: stochastic redistribution, and
  - background contamination: photons are contaminated by the presence of background sources.
- Thus we modify the expected photon counts via

$$\Xi_l(\theta) = \sum_{j \in \mathcal{J}} M_{lj} \Lambda_j(\theta) d_j u(\theta^A, E_j) + \theta_l^B.$$

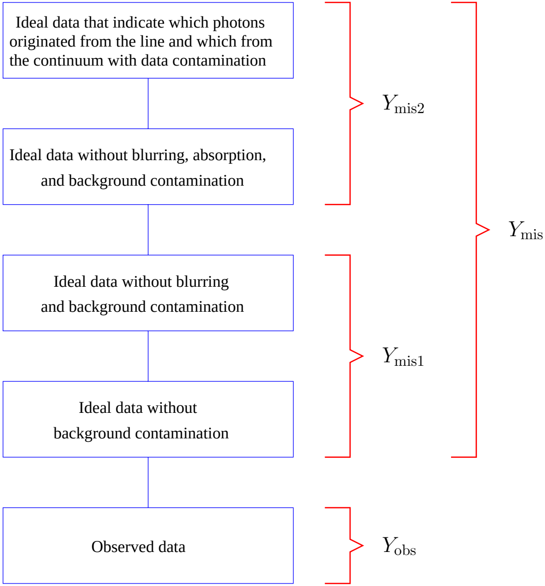
Ideal data that indicate which photons originated from the line and which from the continuum with data contamination
Ideal data without blurring, absorption, and background contamination
Ideal data without blurring and background contamination
Ideal data without background contamination
Observed data
Y_{mis2}
Y_{mis}
Y_{mis1}
Y_{obs}

Hierarchical Structure of Missing Data

- Missing data

  Y_{mis1} : variables that describe blurring, absorption, and background contamination.

  Y_{mis2} : a mixture component indicator variable that indicates which photons originated from the line and which from the continuum.

- Parameters

  ψ : parameters for the continuum, absorption, and background contamination, i.e., $\psi = (\theta^C, \theta^A, \theta^B)$.

  μ : a parameter for the line location.

  ν : a parameter for the line width.

Difficulty with Identifying Narrow Emission Lines

- The standard missing-data algorithm fits the finite mixture problem by iteratively attributing a subset of observed photons to the line and using the mean and variance to update the center and width of the line.
- When a delta function is used to model an emission line, however, the standard algorithm breaks down: The line location does not move from iteration to iteration.
- We suggest fitting the line location without missing data (the mixture indicator).
- This difficulty also persists when the location and width of a Gaussian emission line is simultaneously fitted.

PMG Sampler with a Delta Function Line

(a)

$p(Y_{\text{mis}}|\psi, \mu, Y_{\text{obs}})$

$p(\psi|Y_{\text{mis}}, \mu, Y_{\text{obs}})$

$p(\mu|Y_{\text{mis}}, \psi, Y_{\text{obs}})$

$\xrightarrow{\text{Marginalize}}$

(b)

$p(Y_{\text{mis}}|\psi, \mu, Y_{\text{obs}})$

$p(\psi|Y_{\text{mis}}, \mu, Y_{\text{obs}})$

$p(Y_{\text{mis}}, \mu|\psi, Y_{\text{obs}})$

$\xrightarrow{\text{Permute}}$

(c)

$p(Y_{\text{mis}}, \mu|\psi, Y_{\text{obs}})$

$p(Y_{\text{mis}}|\psi, \mu, Y_{\text{obs}})$

$p(\psi|Y_{\text{mis}}, \mu, Y_{\text{obs}})$

$\xrightarrow{\text{Trim}}$

(d)

$p(\mu|\psi, Y_{\text{obs}})$

$p(Y_{\text{mis}}|\psi, \mu, Y_{\text{obs}})$

$p(\psi|Y_{\text{mis}}, \mu, Y_{\text{obs}})$

$\xrightarrow{\text{Block}}$

(e)

$p(Y_{\text{mis}}, \mu|\psi, Y_{\text{obs}})$

$p(\psi|Y_{\text{mis}}, \mu, Y_{\text{obs}})$

- Our goal is to find a sampler that maintains the transition kernel of an ordinary Gibbs sampler but has quicker convergence than that.

PMG Sampler with a Gaussian Line

(a)

$p(Y_{\text{mis}}|\psi,\mu,\nu,Y_{\text{obs}})$
$p(\psi|Y_{\text{mis}},\mu,\nu,Y_{\text{obs}})$
$p(\mu|Y_{\text{mis}},\psi,\nu,Y_{\text{obs}})$
$p(\nu|Y_{\text{mis}},\psi,\mu,Y_{\text{obs}})$

Marginalize →

(b)

$p(Y_{\text{mis}}|\psi,\mu,\nu,Y_{\text{obs}})$
$p(\psi|Y_{\text{mis}},\mu,\nu,Y_{\text{obs}})$
$p(Y_{\text{mis}},\mu|\psi,\nu,Y_{\text{obs}})$
$p(Y_{\text{mis}},\nu|\psi,\mu,Y_{\text{obs}})$

Permute →

(c)

$p(Y_{\text{mis}},\mu|\psi,\nu,Y_{\text{obs}})$
$p(Y_{\text{mis}},\nu|\psi,\mu,Y_{\text{obs}})$
$p(Y_{\text{mis}}|\psi,\mu,\nu,Y_{\text{obs}})$
$p(\psi|Y_{\text{mis}},\mu,\nu,Y_{\text{obs}})$

Trim →

(d)

$p(\mu|\psi,\nu,Y_{\text{obs}})$
$p(\nu|\psi,\mu,Y_{\text{obs}})$
$p(Y_{\text{mis}}|\psi,\mu,\nu,Y_{\text{obs}})$
$p(\psi|Y_{\text{mis}},\mu,\nu,Y_{\text{obs}})$

Block →

(e)

$p(\mu|\psi,\nu,Y_{\text{obs}})$
$p(Y_{\text{mis}},\nu|\psi,\mu,Y_{\text{obs}})$
$p(\psi|Y_{\text{mis}},\mu,\nu,Y_{\text{obs}})$

- Notice that the resulting sampler is not a blocked version of the ordinary Gibbs sampler!

Results of the EM-type Algorithm

Table: Posterior Modes for μ Identified with the EM-type Algorithm.

line profile	obs-id	mode (keV)	converged starting values (keV)	log posterior
Delta function	47	2.885	0.5 – 6.0	·
	62	2.845	0.5 – 6.0	·
	69	1.805	0.5 – 6.0	·
	70	2.835	0.5 – 6.0	·
	71	2.715	0.5 – 3.7,3.9 – 4.6, and 4.9 – 5.8	1355.31
		5.605	3.8, 4.7 – 4.8, and 5.9 –6.0	1354.90
	1269	2.905	0.5 – 6.0	·
Gaussian function	47	2.765	0.5 – 6.0	·
	62	2.595	0.5 – 6.0	·
	69	2.195	0.5 – 6.0	·
	70	2.705	0.5 – 6.0	·
	71	2.605	0.5 – 6.0	·
	1269	2.575	0.5 – 6.0	·

Posterior Distribution of the Delta Function Line

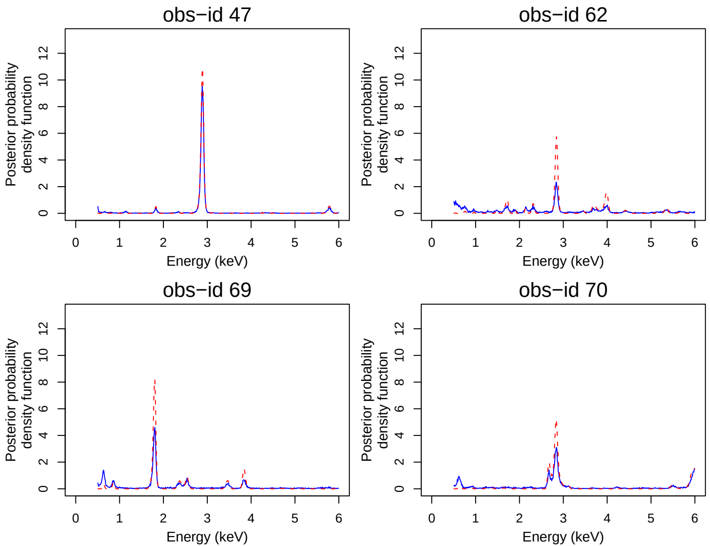

Posterior Distribution of the Delta Function Line

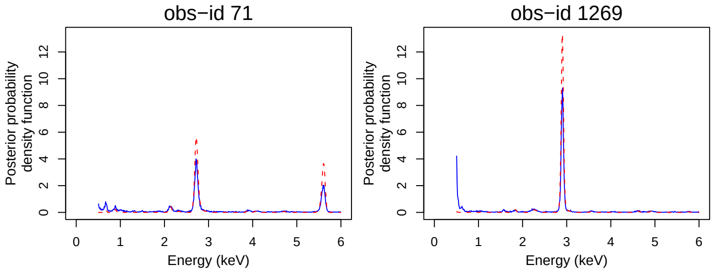

Summary Statistics for the Delta Function Line

observed data set	mode (keV)	HPD region for μ	posterior probability	odds ratio
obs-id 47	2.885	(2.67, 3.07)	83.74%	·
obs-id 62	0.545	(0.50, 1.99)	35.21%	1.74
	2.305	(2.06, 2.43)	9.28%	0.33
	2.845	(2.45, 2.99)	23.78%	·
	3.985	(3.36, 4.10)	15.65%	0.59
obs-id 69	0.625	(0.50, 1.21)	23.64%	·
	1.805	(1.57, 1.97)	39.51%	·
	2.535	(2.20, 2.82)	13.33%	·
	3.835	(3.73, 3.98)	7.10%	·
obs-id 70	0.605	(0.50, 0.99)	13.14%	0.15
	2.845	(2.51, 3.19)	50.82%	·
	5.995	(5.73, 6.00)	14.36%	0.16
obs-id 71	0.665	(0.50, 1.19)	15.41%	0.25
	2.135	(2.02, 2.47)	7.23%	0.11
	2.715	(2.50, 3.07)	41.78%	·
	5.595	(5.36, 5.72)	21.99%	0.39
obs-id 1269	0.505	(0.50, 1.21)	18.25%	0.12
	2.905	(2.75, 3.12)	65.11%	·

Summary Statistics for the Delta Function Line

observed data set	parameter	mean	std. dev.	2.5%	median	97.5%
obs-id 47	λ	34.717	17.668	3.346	34.033	68.927
	α^C	3.4e-4	2.7e-5	3.0e-4	3.4e-4	4.0e-4
	β^C	1.754	0.093	1.577	1.752	1.942
obs-id 62	λ	19.764	23.372	0.610	13.590	92.996
	α^C	3.6e-4	2.9e-5	3.0e-4	3.6e-4	4.2e-4
	β^C	1.769	0.097	1.579	1.769	1.960
obs-id 69	λ	27.354	29.737	1.018	20.809	122.08
	α^C	3.5e-4	3.0e-5	2.9e-4	3.4e-4	4.1e-4
	β^C	1.741	0.098	1.552	1.741	1.935
obs-id 70	λ	24.627	22.578	1.242	20.342	88.06
	α^C	3.2e-4	2.6e-5	2.7e-4	3.2e-4	3.7e-4
	β^C	1.686	0.097	1.498	1.686	1.879
obs-id 71	λ	23.303	19.139	0.993	20.187	65.481
	α^C	4.0e-4	3.4e-5	3.3e-4	3.9e-4	4.7e-4
	β^C	1.826	0.103	1.629	1.825	2.029
obs-id 1269	λ	87.373	214.336	2.358	32.569	782.539
	α^C	2.7e-4	1.9e-5	2.4e-4	2.7e-4	3.1e-4
	β^C	1.985	0.084	1.821	1.985	2.150

Posterior Distribution of the Gaussian Line

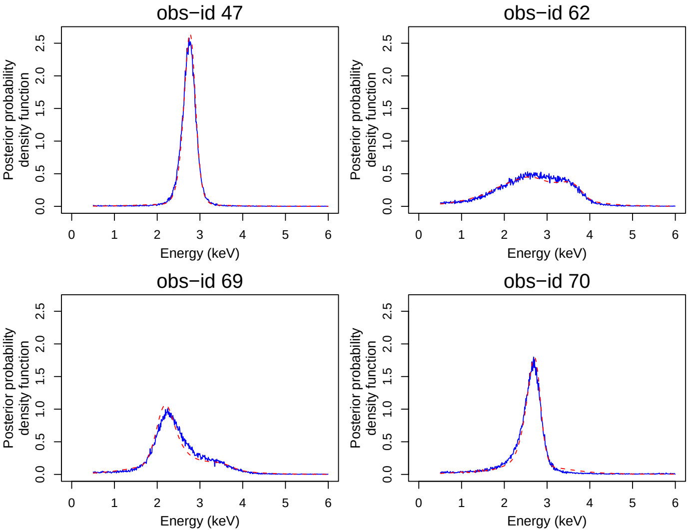

Posterior Distribution of the Gaussian Line

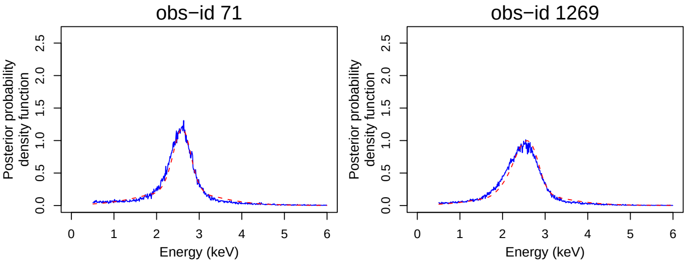

Joint Posterior Distribution of the Gaussian Line

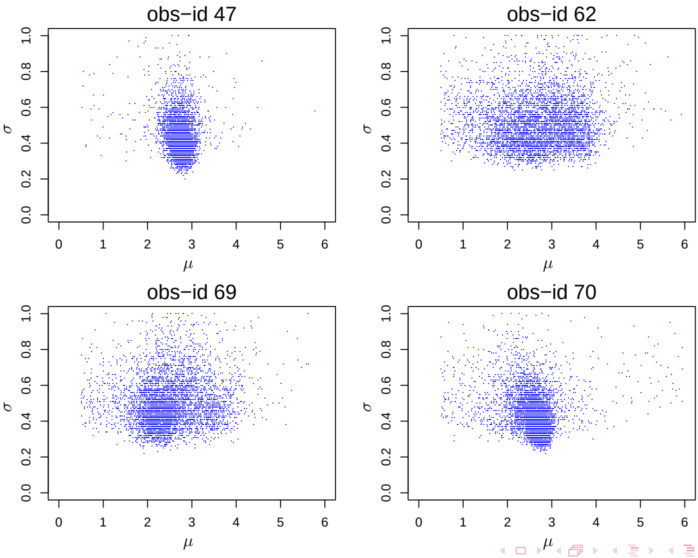

Joint Posterior Distribution of the Gaussian Line

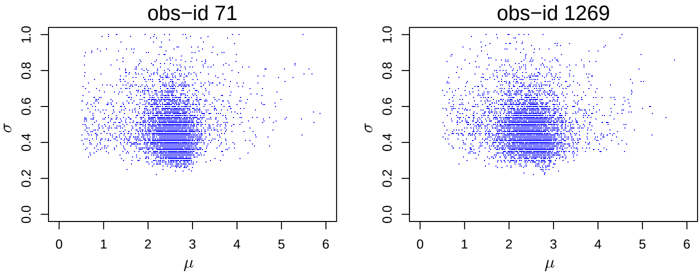

Summary Statistics for the Gaussian Line

observed data set	parameter	mean	std. dev.	2.5%	median	97.5%
obs-id 47	μ	2.733	0.258	2.275	2.745	3.125
	ν	0.197	0.112	0.078	0.168	0.504
	λ	89.401	38.678	18.978	87.139	168.79
	α^C	3.7e-4	2.3e-5	3.4e-4	3.7e-4	4.3e-4
	β^C	1.908	0.087	1.755	1.901	2.095
obs-id 62	μ	2.675	0.813	0.915	2.715	4.075
	ν	0.276	0.158	0.096	0.230	0.723
	λ	35.146	26.774	1.331	29.792	101.544
	α^C	3.8e-4	2.8e-5	3.4e-4	3.8e-4	4.4e-4
	β^C	1.873	0.097	1.708	1.866	2.088
obs-id 69	μ	2.456	0.613	1.245	2.365	3.815
	ν	0.281	0.171	0.096	0.230	0.774
	λ	59.786	40.748	3.589	53.367	155.065
	α^C	3.7e-4	2.7e-5	3.3e-4	3.7e-4	4.3e-4
	β^C	1.864	0.096	1.704	1.855	2.077

Summary Statistics for the Gaussian Line

observed data set	parameter	mean	std. dev.	2.5%	median	97.5%
obs-id 70	μ	2.577	0.528	1.245	2.625	3.485
	ν	0.215	0.128	0.078	0.176	0.578
	λ	59.261	34.128	3.448	57.652	129.735
	α^C	3.5e-4	2.1e-5	3.2e-4	3.5e-4	4.0e-4
	β^C	1.842	0.083	1.697	1.836	2.021
obs-id 71	μ	2.518	0.610	0.985	2.545	3.835
	ν	0.245	0.146	0.090	0.203	0.656
	λ	48.629	33.149	2.522	44.211	123.596
	α^C	4.1e-4	3.5e-5	3.5e-4	4.1e-4	4.9e-4
	β^C	1.913	0.109	1.711	1.909	2.136
obs-id 1269	μ	2.445	0.615	1.095	2.465	3.825
	ν	0.255	0.146	0.090	0.221	0.656
	λ	55.982	42.325	2.085	47.484	155.316
	α^C	2.8e-4	1.9e-5	2.5e-4	2.8e-4	3.2e-4
	β^C	2.032	0.088	1.869	2.030	2.214

Combining All Data Sets

- The six observations of PG 1634+706 were independently observed.
- Under a flat prior distribution, the posterior distribution of the delta function line location given all six data sets is given by

$$
\begin{aligned}
p(\mu|y) &\propto \int \cdots \int \prod_{i=1}^{6} L(\mu, \psi_i | y_i) d\psi_1 \cdots d\psi_6 \\
&= \prod_{i=1}^{6} \int L(\mu, \psi_i | y_i) d\psi_i \\
&= \prod_{i=1}^{6} p(\mu | y_i).
\end{aligned}
$$

Combining All Data Sets

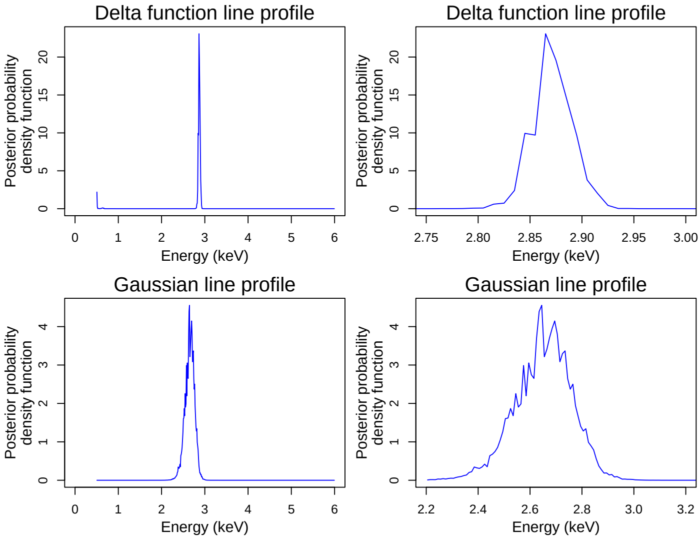

Results of Combining All Data Sets

- The posterior mode of the delta function line location given all data sets is given by 2.865 keV.
- The posterior mean of the Gaussian line location given all data sets is given by 2.667 keV.
- These observed lines are redshifted into 6.69 keV and 6.22 keV in the quasar rest frame, respectively.
- The Fe-K-alpha emission line at 6.69 keV may imply that the iron at the quasar PG 1634+706 was in the ionization state when the quasar is observed.
- On the other hand, if a Gaussian line profile is more appropriate, the Fe-K-alpha line at 6.22 keV seems to indicate neutral iron.